

Highly Conductive Anion Exchange Membrane for High Power Density Fuel-Cell Performance

Xiaoming Ren,^{*,†} Samuel C. Price,[‡] Aaron C. Jackson,[‡] Natalie Pomerantz,[§] and Frederick L. Beyer[‡]

[†]Sensors & Electronic Devices Directorate, U.S. Army Research Laboratory, Adelphi, Maryland 20783, United States

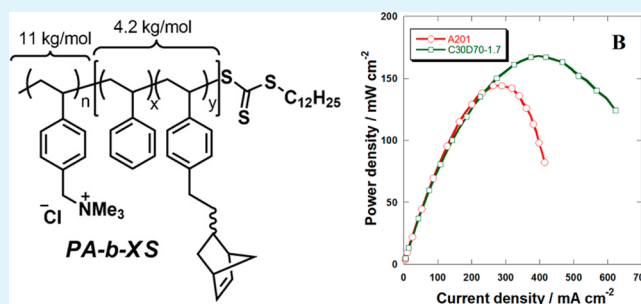
[‡]Weapons & Materials Research Directorate, U.S. Army Research Laboratory, Aberdeen Proving Ground, Aberdeen, Maryland 21005, United States

[§]Natick Soldier Center, U.S. Army NSRDEC, Natick, Massachusetts 01760, United States

Supporting Information

ABSTRACT: Anion exchange membrane fuel cells (AEMFCs) are regarded as a new generation of fuel cell technology that has the potential to overcome many obstacles of the mainstream proton exchange membrane fuel cells (PEMFCs) in cost, catalyst stability, efficiency, and system size. However, the low ionic conductivity and poor thermal stability of current anion exchange membranes (AEMs) have been the key factors limiting the performance of AEMFCs. In this study, an AEM made of styrenic diblock copolymer with a quaternary ammonium-functionalized hydrophilic block and a cross-linkable hydrophobic block and possessing bicontinuous phases of a hydrophobic network and hydrophilic conduction paths was found to have high ionic conductivity at 98 mS cm⁻¹ and controlled membrane swelling with water uptake at 117 wt % at 22 °C. Membrane characterizations and fuel cell tests of the new AEM were carried out together with a commercial AEM, Tokuyama A201, for comparison. The high ionic conductivity and water permeability of the new membrane reported in this study is attributed to the reduced tortuosity of the ionic conduction paths, while the hydrophobic network maintains the membrane mechanical integrity, preventing excessive water uptake.

KEYWORDS: anion exchange membrane, conductivity, water transport, mechanic properties, fuel cell



After decades of R&D, proton exchange membrane fuel cells (PEMFCs) have found practical applications in portable, transportation, and stationary power, usually in niche markets that require high reliability and high efficiency.^{1,2} However, high material cost has prevented the widespread application of PEMFCs.³ The key expense for PEMFCs is the reliance on platinum electrocatalysts, because the strongly acidic environment of the proton exchange membrane limits the stability and performance of other catalytic materials. To overcome the cost and catalyst stability issues, increased attention has been given recently to anion exchange membrane fuel cells (AEMFCs)^{4–7} where non-noble metal catalysts can be used with success. Additionally, non-noble cathodes are more tolerant to contaminants and fuel that crosses through the membrane. To further reduce the cost of AEMFCs, other components such as cell bipolar plates can be stamped out of inexpensive and lighter materials, such as aluminum, instead of being machined from graphite. However, the low ionic conductivity and poor chemical stability of current anion exchange membranes (AEMs) remain the key factors limiting the performance of AEMFCs.^{6,7}

One of the major challenges for polymer electrolyte materials is to balance ionic conductivity with mechanical properties.⁸ Ionic conductivity is typically improved by increasing the ion exchange capacity (IEC), increasing the water swelling level of

the membrane, reducing membrane thickness, or softening the membrane. All of these options reduce the mechanical integrity of the membrane, which can lead to formation of physical holes in the membrane during membrane electrode assembly (MEA) processing and fuel cell operation. Reduced mechanical integrity also leads to excessive water swelling, which may cause the MEA delamination in operation involving humidity cycling. Membranes with two bicontinuous hydrophilic and hydrophobic phases on the order of about 10 nm, such as Nafion and some block copolymer membranes, have been shown to effectively combine high conductivity with mechanical properties.^{9–11} Therefore, in order to maximize both mechanical properties and conductivity, we designed an anion exchange membrane material having poorly ordered, bicontinuous microphase-separated hydrophobic and hydrophilic domains. The hydrophobic domains allow efficient charge transport while the hydrophobic domains provide mechanical toughness. To achieve this morphology, we employed an approach pioneered by Chen, Amendt, and co-workers, with which a reactive diblock copolymer (in this case, PA-b-XS in

Received: June 23, 2014

Accepted: August 5, 2014

Published: August 5, 2014

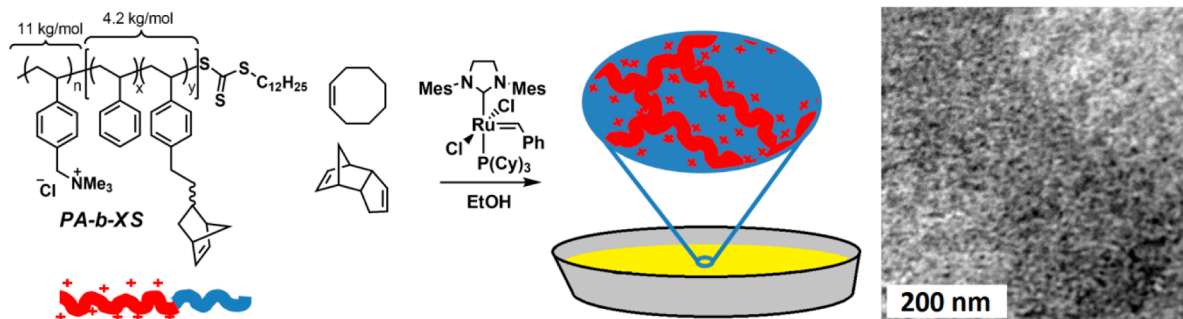


Figure 1. Synthesis of bicontinuous membranes from diblock copolymer PA-*b*-XS. The resulting chemically cross-linked membrane has a disordered and microphase-separated morphology shown in the TEM micrograph on the right.

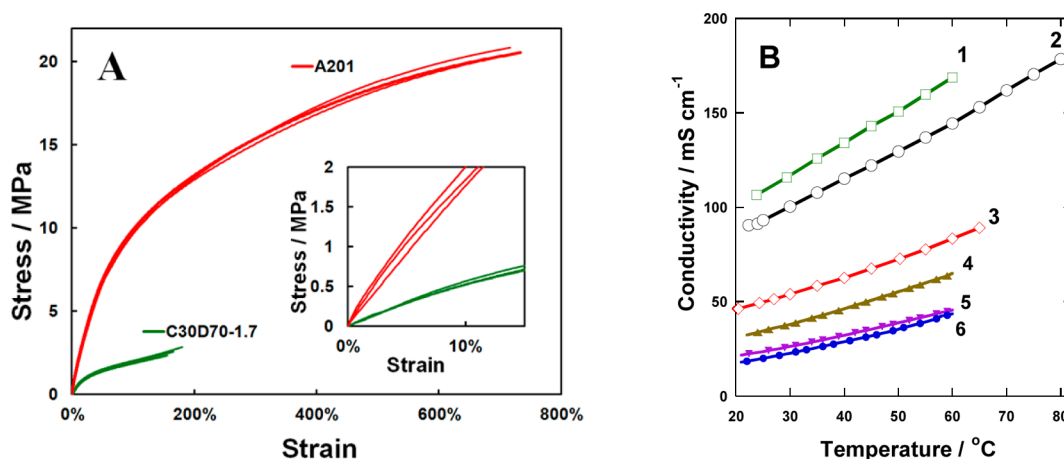


Figure 2. (A) Tensile properties at 80 °C and 85% relative humidity for C30D70-1.7 (green) and Tokuyama A201 (red) membranes. Elastic deformation in the low strain region, displayed on the inset graph, is more applicable to fuel cell operating and fabrication conditions. (B) In-plane conductivity for C30D70-1.7 (curve, counterion: 1, OH⁻; 4, CO₃²⁻; 5, Cl⁻; 6, HCO₃⁻), Tokuyama A201 (3, OH⁻), and Nafion-117 membranes (2, H⁺).

Figure 1) is incorporated into a cross-linking film during casting.^{12,13}

In our initial report using this membrane formation technique, low-molecular-weight block copolymers were used, targeting small domain sizes reported to have high conductivity.¹⁴ However, these materials lacked the requisite mechanical properties for fuel cell application, and the domain size was controlled more by the cross-linking reaction kinetics rather than by the molecular weight of the polymer. In this report we have increased the molecular weight of the diblock copolymer from 7.3 to 14.2 kg mol⁻¹, and increased the rate of the cross-linking reaction (by increasing the concentration and DCPD:COE ratio). The resulting membrane retains the disordered but bicontinuous, phase-separated morphology of the earlier materials, as confirmed by small-angle X-ray scattering, and TEM (see the Supporting Information). The mechanical properties of the resulting membrane (C30D70-1.7) were improved, together with reduced membrane swelling when compared at the same IEC. A comparison of the membrane mechanical properties between C30D70-1.7 and Tokuyama A201 is shown in Figure 2A.

Fortuitously, the membrane conductivity also increased, even though the domain size was roughly consistent with smaller molecular weight PA-*b*-XS. We attribute the increase in conductivity to an increase in the continuity of the ionic phase. In our previous report, only 54–72% of the hydroxide ions cast into the membrane were detectable by titration.¹⁴ By increasing the molecular weight of the diblock copolymer, the

C30D70-1.7 membranes in this report have 92% of the ions detectable by titration, indicating that 92% of the ionic domains are continuous. This high degree of continuity results in a hydroxide conductivity of 98.4 mS cm⁻¹ at room temperature when in contact with liquid water, which is higher than any other hydroxide conducting membrane measured and reported in literature.⁷ Additionally, the activation energy for the ionic transport in both Nafion-117 and C30D70-1.7 membranes is very low at 10.4 kJ mol⁻¹, which may indicate that the transport of some hydroxide ions in the AEM pore solution could occur through a reverse Grotthuss proton hopping mechanism.

Also of note, the anion exchange membrane ionic conductivity is very sensitive to the particular counterion distribution in the membrane.^{15,16} It is well-known that carbon dioxide in the air slowly equilibrates with hydroxide ions in solution to yield carbonate and bicarbonate ions, which then move into the membrane. This effect is seen in Figure 2B for the ionic conductivity measured for various counterions, and because of this, extreme care is required to minimize/eliminate CO₂ exposure of the membrane before and during the conductivity measurement. Fuel cells operated with pure H₂/O₂ feeds have shown that the initial carbonates in the AEM can be effectively displaced by the OH⁻ ions produced at the cell cathode, a phenomenon of self-purging.¹⁷ The counterion forms of the AEMs under measurements were verified by titration experiments, and the stability of the membrane ionic conductivity by extended test duration, both detailed in the Supporting Information.

Table 1. Characteristics of the C30D70-1.7 Alkaline Exchange Membrane and Two Commercial Membranes for Fuel Cell Applications

membrane (counterion)	IEC (mequiv g ⁻¹)	water uptake (mass %)	0.2% offset yield point ^a (MPa)	conductivity, wet at 22 °C (mS cm ⁻¹)	pore ion concentration (mol L ⁻¹)	tortuosity factor (N/A)	transport activation energy (kJ mol ⁻¹)
C30D70-1.7 (OH ⁻)	1.65 ± 0.05	117 ± 2%	0.55 ± 0.16	98.4 ± 3.1	1.4 ± 0.1	1.6 ± 0.1	10.4
Tokuyama A201 (OH ⁻)	1.68 ± 0.08	44 ± 5%	1.64 ± 0.31	45.8 ± 1.5	4.1 ± 0.4	6.4 ± 0.7	12.2
Nafion-117 (H ⁺)	0.91	26% ^b	~0.5 ^b	90.6	2.6	4.5	10.4

^aCalculated from stress vs strain curves collected at 80 °C at 85% relative humidity, on membranes in the chloride form. ^bFrom Figure 9 in ref 18, collected on Nafion-117 submersed in water at 80 °C in the proton form. Error is the 95% confidence interval.

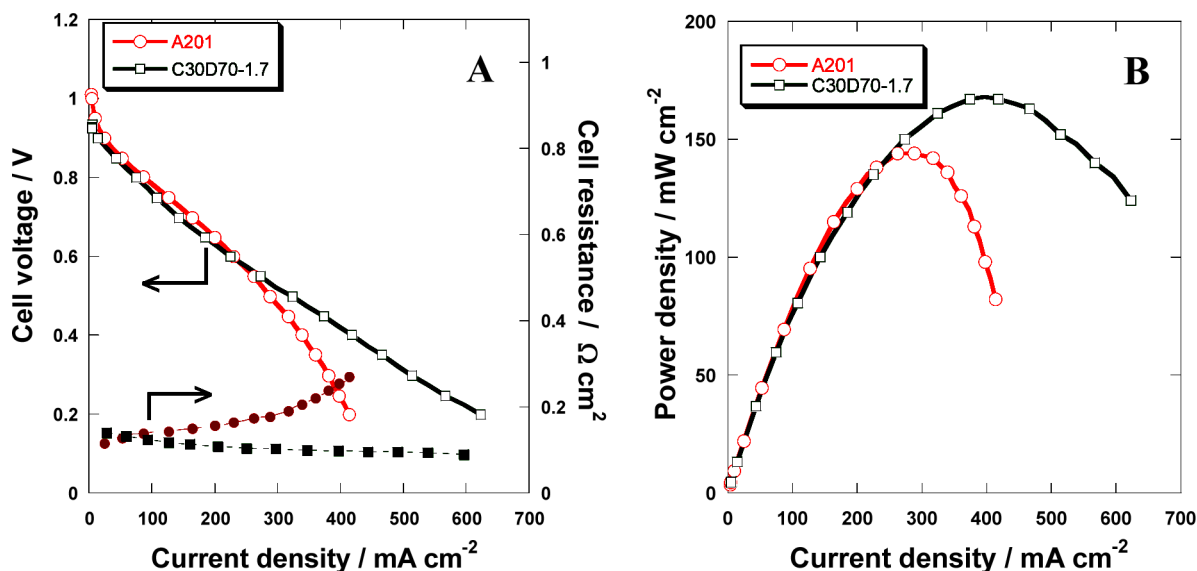


Figure 3. (A) Comparison of H₂/air fuel cell VI polarization curve (left axis) and cell resistance (right axis) at 50 °C for the two MEAs made with Tokuyama A201 and C30D70-1.7 AEMs. (B) Comparison of H₂/air fuel cell power densities as a function of cell current density at 50 °C.

Table 1 displays the performance characteristics of the C30D70-1.7 membrane in comparison to Tokuyama A201 (an alkaline exchange membrane) and Nafion-117 (a proton exchange membrane). Under the assumption of volume additivity, the ionic conductivity of a polymer electrolyte membrane is approximated by eq 1,¹⁹

$$\sigma_{\text{memb}} = \frac{1}{\tau} \lambda c_i \varepsilon \quad (1)$$

where τ is the tortuosity factor, λ is effective molar conductance in bulk aqueous solution, c_i is the molar concentration of counterion in the membrane hydrophilic pores, and ε is the hydrophilic pore volume fraction. Effective molar conductances for H⁺ and OH⁻ in a bulk aqueous solution are calculated, according to Reijenga and Kennler, by eq 2,²⁰

$$\lambda = F \mu_0 e^{(-0.5I^{0.5} Z^{-1.78})} \quad (2)$$

where F is the Faraday constant, I is the ionic strength in the membrane pores, Z the ionic charge, and μ_0 the counterion mobility at infinitely diluted aqueous solution (36.25 and 20.6 ($\times 10^{-8}$ m² v⁻¹ s⁻¹) for H⁺ and OH⁻ at 298 K, respectively). From measurement results of water uptake (WU), IEC, and membrane conductivity measurements, the tortuosity factor of counterion conduction paths is estimated according to eq 1, and these results are listed in Table 1. The very low tortuosity factor for the C30D70-1.7 membrane simply arises from the

large volume fraction of water in the membrane and the bicontinuous membrane morphology.

The fuel-cell performance of a thin C30D70-1.7 membrane (55 μm) is compared to that of a Tokuyama A201 membrane (28 μm) under otherwise identical fuel cell preparation and test conditions in Figure 3. The cell with the C30D70-1.7 membrane shows a higher peak power density at 168 mW cm⁻², compared to that of the Tokuyama membrane at 148 mW cm⁻². The better fuel-cell performance of the C30D70-1.7 membrane likely originates from its higher conductivity and faster water transport within the membrane. As the current density increases, the resistance of the cell with Tokuyama A201 membrane increases, which is indicative of the cathode drying-out from water consumption by the oxygen reduction reaction and from water electro-osmotic drag induced by OH⁻ migration toward anode.²¹ In comparison, at the high current region, the resistance of the cell with the C30D70-1.7 membrane is stable, indicating the cell cathode remains hydrated by the high water permeability within the membrane. Separate measurements on water permeability through the two membranes, detailed in the Supporting Information, confirm the much higher water permeability in C30D70-1.7 at 4.4×10^{-6} g cm⁻¹ s⁻¹ atm⁻¹ at 45 °C as compared with that of Tokuyama A201 at 2.9×10^{-6} g cm⁻¹ s⁻¹ atm⁻¹ at the same temperature.

In conclusion, the bicontinuous AEM morphology consisting of hydrophobic polymer framework and hydrophilic ionic conduction paths is responsible for the high anionic conductivity of C30D70-1.7 (168 mS cm⁻¹ at 60 °C) with restricted membrane swelling. The C30D70-1.7 membrane also has a high water permeability. Both high conductivity and water permeability are attributed to a high level of continuity and low tortuosity in the membrane's ionic conduction paths. The peak power density of the fuel cell using C30D70-1.7 membrane is superior to that using the Tokuyama A201 membrane.

■ ASSOCIATED CONTENT

■ Supporting Information

Detailed synthetic procedures for PA-*b*-XS, and experimental conditions used for membrane characterizations and fuel cell tests. This material is available free of charge via the Internet at <http://pubs.acs.org/>.

■ AUTHOR INFORMATION

Corresponding Author

*E-mail: xiaoming.ren.civ@mail.mil.

Notes

The authors declare no competing financial interest.

■ ACKNOWLEDGMENTS

S.C.P. and A.C.J. were supported by the Postgraduate Research Participation Program at the U.S. Army Research Laboratory, administered by the Oak Ridge Institute of Science and Education through an interagency agreement between the U.S. Department of Energy and Army Research Laboratory (Contract ORISE 1120-1120-99).

■ REFERENCES

- (1) Wang, Y.; Chen, K. S.; Mishler, J.; Cho, S. C.; Adroher, X. C. A Review of Polymer Electrolyte Membrane Fuel Cells: Technology, Applications, and Needs on Fundamental Research. *Appl. Energy* **2011**, *88*, 981–1007.
- (2) Peighambaroust, S. J.; Rowshanzamir, S.; Amjadi, M. Review of the Proton Exchange Membranes for Fuel Cell Applications. *Int. J. Hydrogen Energy* **2010**, *35*, 9349–9384.
- (3) Calay, R. K.; Mustafa, M. Y.; Mustafa, M. F., Challenges Facing Hydrogen Fuel Cell Technology to Replace Combustion Engines. In *Applied Energy Technology, Parts 1 and 2*, Wang, A., Che, L. K., Dong, R., Zhao, G., Eds.; Trans Tech Publications: Dürnten, Switzerland, 2013; Vol. 724–725, pp 715–722.
- (4) Lu, S.; Pan, J.; Huang, A.; Zhuang, L.; Lu, J. Alkaline Polymer Electrolyte Fuel Cells Completely Free from Noble Metal Catalysts. *Proc. Natl. Acad. Sci. U.S.A.* **2008**, *105*, 20611–20614.
- (5) Varcoe, J. R.; Slade, R. C. T. Prospects for Alkaline Anion-Exchange Membranes in Low Temperature Fuel Cells. *Fuel Cells* **2005**, *5*, 187–200.
- (6) Hickner, M. A.; Herring, A. M.; Coughlin, E. B. Anion Exchange Membranes: Current Status and Moving Forward. *J. Polym. Sci., Part B: Polym. Phys.* **2013**, *51*, 1727–1735.
- (7) Merle, G.; Wessling, M.; Nijmeijer, K. Anion Exchange Membranes for Alkaline Fuel Cells: A Review. *J. Membr. Sci.* **2011**, *377*, 1–35.
- (8) Elabd, Y. A.; Hickner, M. A. Block Copolymers for Fuel Cells. *Macromolecules* **2010**, *44*, 1–11.
- (9) Chen, L.; Hallinan, D. T.; Elabd, Y. A.; Hillmyer, M. A. Highly Selective Polymer Electrolyte Membranes from Reactive Block Polymers. *Macromolecules* **2009**, *42*, 6075–6085.
- (10) Bae, B.; Miyatake, K.; Watanabe, M. Synthesis and Properties of Sulfonated Block Copolymers Having Fluorenyl Groups for Fuel-Cell Applications. *ACS Appl. Mater. Interfaces* **2009**, *1*, 1279–1286.

(11) Ding, J.; Chuy, C.; Holdcroft, S. A Self-organized Network of Nanochannels Enhances Ion Conductivity through Polymer Films. *Chem. Mater.* **2001**, *13*, 2231–2233.

(12) Chen, L.; Phillip, W. A.; Cussler, E. L.; Hillmyer, M. A. Robust Nanoporous Membranes Templated by a Doubly Reactive Block Copolymer. *J. Am. Chem. Soc.* **2007**, *129*, 13786–13787.

(13) Amendt, M. A.; Chen, L.; Hillmyer, M. A. Formation of Nanostructured Poly(dicyclopentadiene) Thermosets Using Reactive Block Polymers. *Macromolecules* **2010**, *43*, 3924–3934.

(14) Price, S. C.; Ren, X. M.; Jackson, A. C.; Ye, Y. S.; Elabd, Y. A.; Beyer, F. L. Bicontinuous Alkaline Fuel Cell Membranes from Strongly Self-Segregating Block Copolymers. *Macromolecules* **2013**, *46*, 7332–7340.

(15) Grew, K. N.; Ren, X. M.; Chu, D. R., Effect of CO₂ on the Alkaline Membrane Fuel Cell. In *Polymer Electrolyte Fuel Cells 11*, Gasteiger, H. A., Weber, A., Narayanan, S. R., Jones, D., Strasser, P., SwiderLyons, K., Buchi, F. N., Shirvanian, P., Nakagawa, H., Uchida, H., Mukerjee, S., Schmidt, T. J., Ramani, V., Fuller, T., Edmundson, M., Lamy, C., Mantz, R., Eds.; ECS Transactions Series; The Electrochemical Society: Pennington, NJ, 2011; Vol. 41, pp 1979–1985.

(16) Suzuki, S.; Muroyama, H.; Matsui, T.; Eguchi, K. Influence of CO₂ Dissolution into Anion Exchange Membrane on Fuel Cell Performance. *Electrochim. Acta* **2013**, *88*, 552–558.

(17) Siroma, Z.; Watanabe, A.; Yasuda, K.; Fukuta, K.; Yanagi, H., Mathematical Modeling of the Concentration Profile of Carbonate Ions in an Anion Exchange Membrane Fuel Cell. In *Polymer Electrolyte Fuel Cells 10, Pts 1 and 2*, Gasteiger, H. A.; Weber, A.; Strasser, P.; Edmundson, M.; Lamy, C.; Darling, R.; Uchida, H.; Schmidt, T. J.; Shirvanian, P.; Buchi, F. N.; Mantz, R.; Zawodzinski, T.; Ramani, V.; Fuller, T.; Inaba, M.; Jones, D.; Narayanan, S. R., Eds. **2010**; Vol. 33, 1935–1943.

(18) Kundu, S.; Simon, L. C.; Fowler, M.; Grot, S. Mechanical Properties of Nafion Electrolyte Membranes under Hydrated Conditions. *Polymer* **2005**, *46*, 11707–11715.

(19) Knauth, P.; Sgreccia, E.; Donnadio, A.; Casciola, M.; Di Vona, M. L. Water Activity Coefficient and Proton Mobility in Hydrated Acidic Polymers. *J. Electrochem. Soc.* **2011**, *158*, B159–B165.

(20) Reijenga, J. C.; Kenndler, E. Computational Simulation of Migration and Dispersion in Free Capillary Zone Electrophoresis 0.1. Description of the Theoretical-Model. *J. Chromatogr. A* **1994**, *659*, 403–415.

(21) Eikerling, M.; Kharkats, Y. I.; Kornyshev, A. A.; Volkovich, Y. M. Phenomenological Theory of Electro-osmotic Effect and Water Management in Polymer Electrolyte Proton-Conducting Membranes. *J. Electrochem. Soc.* **1998**, *145*, 2684–2699.